β-delayed neutron emission of ^{64}Mn, ^{62}Cr, and ^{65}Fe

W.-J. Ong,[1,2,3,*] H. Schatz [2,3,4] K. Kravvaris [1] S. Ahn [4,5,†] K. Childers,[3,6,‡] B. P. Crider,[7]
A. C. Dombos [2,3,4] C. Langer,[8,§] R. Lewis,[3,6] S. N. Liddick,[3,6] S. Lyons [3,4] Z. Meisel [4,9] F. Montes,[3,4]
J. Pereira,[3,4] D. Richman,[2,10] K. Schmidt [3,4,11] and A. Spyrou [2,3,4]

[1]*Nuclear and Chemical Sciences Division, Lawrence Livermore National Laboratory, Livermore, California 94550, USA*
[2]*Department of Physics and Astronomy, Michigan State University, East Lansing, Michigan 48824, USA*
[3]*Facility for Rare Isotope Beams, Michigan State University, East Lansing, Michigan 48824, USA*
[4]*Joint Institute for Nuclear Astrophysics–Center for the Evolution of the Elements,*
Michigan State University, East Lansing, Michigan 48824, USA
[5]*Cyclotron Institute, Texas A&M University, College Station, Texas 77843, USA*
[6]*Department of Chemistry, Michigan State University, East Lansing, Michigan 48824, USA*
[7]*Department of Physics and Astronomy, Mississippi State University, Mississippi State, Mississippi 39762, USA*
[8]*Institute for Applied Physics, Goethe-University Frankfurt a. M., Frankfurt am Main 60438, Germany*
[9]*Department of Physics and Astronomy, Ohio Univeristy, Athens, Ohio 45701, USA*
[10]*Los Alamos National Laboratory, Los Alamos, New Mexico 87545, USA*
[11]*Institute of Radiation Physics, Helmholtz-Zentrum Dresden-Rossendorf, Dresden 01328, Germany*

The β-decay properties of nuclei near the second nuclear "island of inversion" around neutron rich nuclei with neutron number 40 are important tests of nuclear structure models and interactions. In particular, the β-delayed neutron emission branch (P_n), is useful for investigating β-strength and neutron-γ competition above the neutron separation energies of the daughter nuclei. We report new constraints for P_n values for three nuclei in the region: ^{62}Cr ($P_n < 1\%$), ^{64}Mn ($P_n = 1.5(6)\%$), and ^{65}Fe ($P_n < 1\%$), measured with the Neutron Emission Ratio Observer (NERO) neutron long counter system and the Beta Counting Station (BCS) at the National Superconducting Cyclotron Laboratory (NSCL). Our results resolve the large discrepancy between previous direct and indirect measurements for ^{64}Mn and confirm the predictions of global theoretical models when a statistical treatment of the γ and neutron decays of the daughter states is included. We also obtain improved half-lives for ^{62}Cr [206(5) ms] and the short-lived isomer in the ^{62}Fe daughter [112(7) ms] from β-delayed γ emission data obtained in the same experiment with the Summing NaI (SuN) total absorption spectrometer. Finally, we use γ emission data to obtain a new upper limit for the ^{62}Cr β-decay population of the long-lived isomeric state in ^{62}Mn.

I. INTRODUCTION

The Cr–Fe nuclei with neutron numbers around $N = 40$ mark a so-called "island of inversion" characterized by substantial deformation and complex neutron configurations involving both the fp shell as well as the $g_{9/2}$ and $d_{5/2}$ orbitals [1]. These nuclei can therefore serve as probes for the (nuclear interaction driven) evolution of shell gaps as neutrons are added towards $N = 40$, thus increasing the role of configurations that involve the deformation-driving $g_{9/2}$ orbital. Indeed,

γ-spectroscopy and $B(E2)$ measurements of the Fe isotopic chain indicate an increase in collectivity already at ^{64}Fe [2–4]. Shell model calculations have shown that inclusion of the $g_{9/2}$ orbital is essential to describe the structure of ^{64}Fe, with typical orbital population of 60% [3,4], giving this nucleus a special role in the transition to the $N = 40$ island of inversion.

The shell structure of ^{64}Fe can also be probed through the β decay of ^{64}Mn, which has been shown to have a 1+ ground state [5]. For example, a significant occupation of the $\nu g_{9/2}$ neutron configurations would reduce the role of the dominant $\nu f_{5/2} \rightarrow \pi f_{7/2}$ allowed transitions [2]. In this context, the finding of an unexpectedly large ^{64}Mn β-delayed neutron branch of $P_n = 33(2)\%$ is notable [6,7]. This measurement was performed by direct detection of neutrons exhibiting the correct half-life of ^{64}Mn using a neutron long counter and is about an order of magnitude larger than $P_n = 2\%$ predicted by theory [8]. However, an indirect measurement employing β-delayed γ-ray spectroscopy obtained a value of $P_n = 2.7(6)\%$, in line with theoretical expectations, by using the
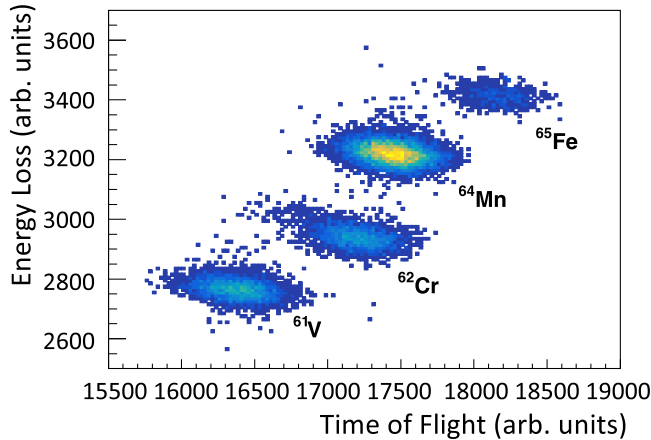
FIG. 1. Momentum-corrected particle identification plot showing energy loss ΔE in arbitrary units vs time of flight also in arbitrary units for each ion implanted into the DSSD.

FIG. 2. Best fit of the time distribution of detected beta particles correlated with a ^{64}Mn implant. Data are shown by the red histogram, overlaid with the total fit (black solid line), ^{64}Mn decays (blue dashed line), daughter ^{64}Fe decays (red dashed line), and neutron daughter ^{63}Fe decays (green dashed line). The inset shows the neutron-gated decay curve, with the data (red histogram), background (grey dashed histogram), fit of the data (red solid line), and fit of the background (black dashed line).

995 keV γ ray from the ground state decay of the β-delayed neutron daughter ^{63}Fe to ^{63}Co [9].

Here we address this discrepancy by performing a new direct measurement of the ^{64}Mn β-delayed neutron emission using the NERO long-counter. This is not only important for understanding the nuclear structure near $N = 40$, but an accurate P_n is also needed to obtain absolute decay branches and strength functions from a total absorption spectroscopy study [10]. In addition, the large P_n observed in Ref. [6] is also an order of magnitude larger than predictions from global QRPA models [8,11] that are used in astrophysical model calculations of the r process and neutron star crusts. A confirmed P_n value is therefore also important for astrophysical applications providing a test of the validity of the theoretical models used. We also report the first measurements of the β-delayed neutron branches of ^{62}Cr and ^{65}Fe.

II. EXPERIMENT DETAILS

The experiment was performed at the National Superconducting Cyclotron Laboratory (NSCL) at Michigan State University. A 35 p nA ^{82}Se beam with an energy of 140 MeV/u was impinged on a 352 mg/cm^2 beryllium target; the resultant mixture of nuclides was purified using the A1900 fragment separator with a momentum spread $\Delta p/p$ of 2%, such that the composition of the cocktail beam transmitted to the experimental end station consisted almost entirely of ^{61}V (24%), ^{62}Cr (19%), ^{64}Mn (51%), and ^{65}Fe (6%). For the momentum-corrected particle identification plot see Fig. 1.

Beam particles were identified using the ΔE-TOF (time of flight) method, with the energy loss taken from a 525-μm-thick Si PIN detector located at the beginning of the end station, and the time of flight calculated from the time difference between an I2 scintillator at the image position of the A1900 and the PIN detector.

The experimental end station for the β-delayed neutron measurement consisted of (in order, from upstream to downstream) (1) a stack of two Si PIN detectors and an Al degrader on a rotating holder that allowed for varying the degrader
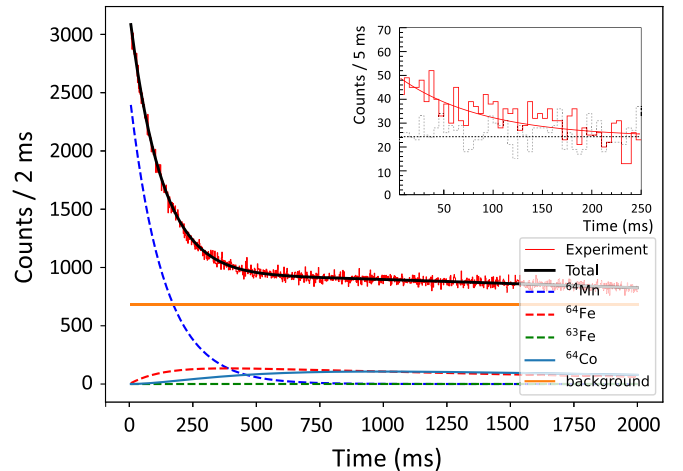
thickness; (2) the Summing NaI detector (SuN); and (3) the Beta Counting Station (BCS) [12] housed in the bore of the NERO detector [13]. The beam was implanted in a 979-μm thick double-sided silicon strip detector (DSSD) as part of the BCS. Neutrons detected by NERO in the 200 μs following a decay event were considered to be associated with the β decay. In addition, data for β-delayed γ emission were taken separately, stopping the beam upstream in the center of SuN using a smaller DSSD. Further experimental details can be found in [14].

III. RESULTS

In this work, we report extracted β-decay half-lives ($T_{1/2}$) as well as the strength of the β-delayed neutron emission branch (P_n) extracted from NERO data for three isotopes: ^{64}Mn, ^{62}Cr, and ^{65}Fe. Additionally, by including data from the SuN detector, we further interpret the possible outcomes of the ^{62}Cr decay. NERO and SuN results from the decay of ^{61}V were previously published [14,15] and are thus omitted from this paper. To provide an assessment of the uncertainties arising from the experiment statistics and specific daughter properties, a Markov chain Monte Carlo (MCMC) method was used.

A. ^{64}Mn

As all possible decay products of ^{64}Mn have a negative β-delayed neutron emission Q value ($Q_{\beta-n}$), the neutron emission-gated decay curve of ^{64}Mn must be entirely from decays of ^{64}Mn. The neutron-gated decay curve fit (inset of Fig. 2) gives a half-life of $T_{1/2} = 91(6)$ ms. After subtraction of the flat background obtained from time-reversed correlations and using the scaled flat efficiency of 37(5)% determined
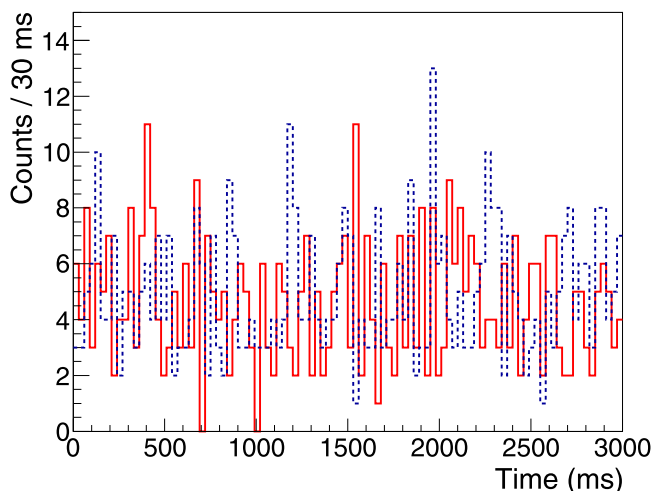
FIG. 3. Neutron-gated decay curve of ^{62}Cr (red solid histogram) and neutron-gated background (grey dashed histogram).

in [13,14], a P_n of 1.5(6)% is obtained. The large error is mainly due to the systematic uncertainty in the efficiency of NERO and the statistical uncertainty from the low number of counts of β-delayed neutron events.

The full ^{64}Mn β-decay curve was also constructed by fitting the decays of the parent ^{64}Mn, the daughter ^{64}Fe (with $T_{1/2} = 2.0(2)$ s [7]), granddaughter ^{64}Co ($T_{1/2} = 0.3(1)$ s), and neutron daughter ^{63}Fe (with $T_{1/2} = 6.1(6)$ s [16]) (Fig. 2). The MCMC analysis of the ungated decay curve, using a Gaussian prior of 1.5(6)% from the separately measured P_n from this work, a ^{64}Mn half-life of 92.1(8) ms was obtained, more precise but in good agreement with the ENSDF database weighted average from previous work of 90(2) ms [7].

B. ^{62}Cr

The β-delayed neutron decay curve for ^{62}Cr is consistent with background (Fig. 3). Taking into account the statistical uncertainty and the uncertainty in the efficiency of NERO, we obtain an upper limit of 1% for the P_n for ^{62}Cr. No previous measured P_n has been reported, but a previous calculation gives a P_n of 1%, consistent with our result [17]. The interpretation of the ^{62}Cr β-particle decay curve is further complicated by the fact that the half-life of the ^{62}Mn daughter is disputed. Studies of the decay of ^{62}Cr, similar to this study, have reported the need of a 92(13) ms [18,19] ^{62}Mn daughter half-life in order to reproduce the observed ^{62}Cr β-particle decay curve. An earlier study [20] produced ^{62}Mn directly via a ^{76}Ge beam impinging on a tungsten target and determined a much longer half-life of 880(150) ms from β particles and β-delayed γ rays. Hannawald *et al.* [2] produced ^{62}Mn through proton spallation on a uranium target and determined a half-life of 671(5) ms from β-delayed neutrons. The analysis of β-particle decay curves from the same experiment [6] confirms the long half-life obtained from the neutron data, but indicates in addition also the presence of a 84(10) ms short-lived component. To explain these results, Gaudefroy *et al.* [18] proposed the existence of two β-decaying states in ^{62}Mn: a short lived $T_{1/2} = 92(13)$ ms low-spin state directly populated by the decay of ^{62}Cr with a branching of 73(5)% and a small P_n value, and a separate higher-spin state with $T_{1/2} = 671(5)$ ms and a substantial P_n value.

The γ-ray data taken with SuN in this experiment allows for a much better constrained analysis of the decays of ^{62}Cr and ^{62}Mn. Our statistics and the γ efficiency of the SuN total absorption spectrometer are sufficient to determine the ^{62}Cr half-life independently of the ^{62}Mn half-life.

The SuN detector is a high-efficiency summing NaI barrel consisting of eight half-annular segments [21]. The high efficiency and segmentation of SuN allows for $\gamma - \gamma$ coincidences to be easily associated with the total energy of the γ-decaying state. Gating the β-particle decay curve on the 355–285 keV γ-ray cascade [2,22] [labeled (a) in the top panel of Fig. 4] in the total absorption spectrum results in a half-life of 206(5) ms [top plot (i) of bottom panel of Fig. 4].

Other than the 877 keV γ ray produced from the de-excitation of the first excited state of ^{62}Fe, the proposed long-lived isomer and the short-lived isomer have not been identified to share any other γ rays. The work of [18] reported a previously unobserved 815 keV γ ray, in coincidence with the 877 keV γ ray. The γ-TAS coincidence plot from the present study shows the same γ-ray cascade [labeled (b) in the top panel of Fig. 4]. Gating on the cascade allows the determination of the half-life of the shorter-lived isomer of ^{62}Mn of 112(7) ms [middle plot (ii) of bottom panel of Fig. 4].

In principle one can search for evidence of a long-lived 671(5) ms component in the ^{62}Cr decay curve. Previously the unknown P_n of ^{62}Cr would have complicated such a search, because the neutron daughter ^{61}Mn has a very similar reported half-life $T_{1/2} = 709(15)$ ms. This would have led to degeneracies in the free parameters. With the small P_n limit from this work we can now attempt such a search to constrain the possible feeding of the long component via the β decay of ^{62}Cr.

For the fit of the ^{62}Cr β-particle decay curve we employed a MCMC approach. In addition to the parent ^{62}Cr decay [using a Gaussian prior of 206(5) ms], the shorter-lived ^{62}Mn daughter decay [using a Gaussian prior of 112(7) ms], where both priors were determined from the γ-gated fits, and a flat background, the fit also included a longer-lived daughter component (using a flat prior of 0–1000 ms). The posterior distribution, shown in Fig. 5, shows that the fit half-lives of both ^{62}Cr and the shorter-lived ^{62}Mn component are largely independent of the isomer activity. Using this approach, we found that we could only constrain the total isomer activity, but not the half-life and fraction of the ^{62}Mn isomer separately.

Performing fits with the isomer fraction and half-life as independent variables results in an almost flat posterior probability distribution for the isomer half-life, which suggests that no meaningful constraint can be placed on the population of the long-lived ^{62}Mn isomer by ^{62}Cr decay from this decay curve. A fit with a 25% long component and a half-life of 620 ms results in only a slightly improved $\chi^2/\text{dof} = 1.05$, compared to $\chi^2/\text{dof} = 1.16$ without any long component and the shallowness of the χ^2 curve indicates that the isomer population is consistent with both 0% and 100%.
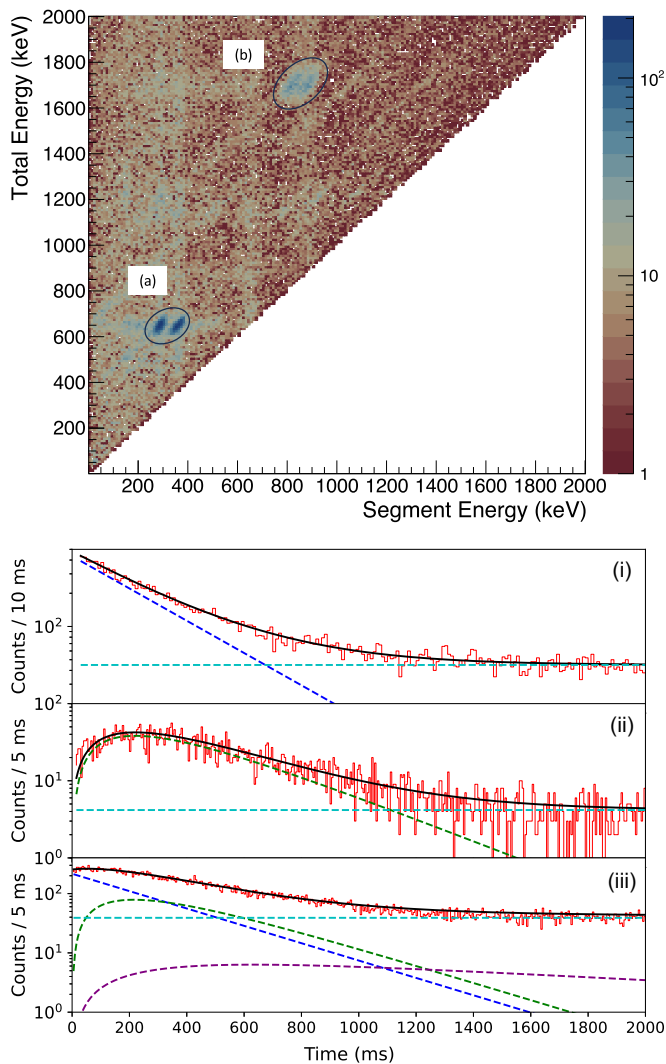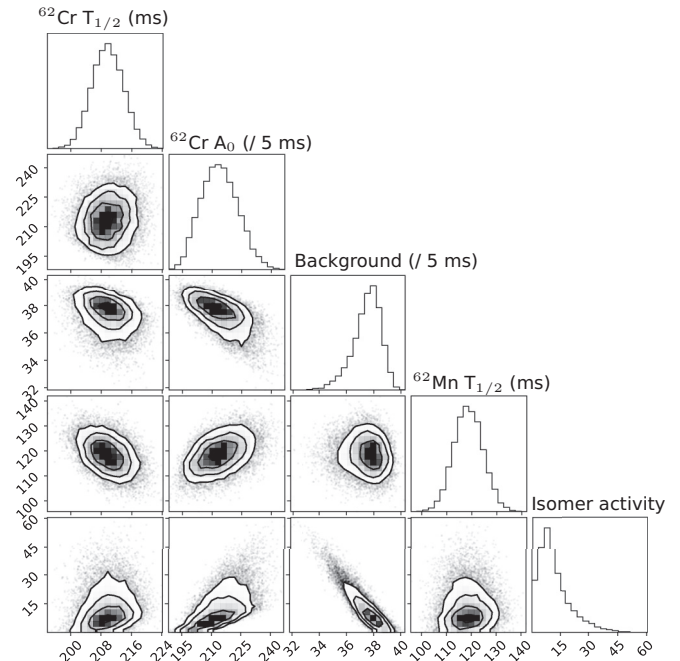
FIG. 5. MCMC results showing the correlations between the free parameters. From the top row to the bottom: (1) ^{62}Cr $T_{1/2}$, (2) implanted ^{62}Cr activity, (3) background, (4) short-lived ^{62}Mn $T_{1/2}$, (5) long-lived ^{62}Mn activity. The posterior distributions give 206(5) and 111(6) ms respectively for the half-lives of ^{62}Cr and the short-lived ^{62}Mn daughter decay. The implanted ^{62}Cr activity and background are given in counts per 5 ms.

FIG. 4. Top: Energy recorded in a single NaI crystal (keV) vs total energy in SuN (keV). The ellipse marked (a) is the 355–285 keV coincidence from the decay of ^{62}Cr and the upper ellipse marked (b) is the 815–877 keV coincidence from the decay of the shorter-lived β-decay isomer of ^{62}Mn. The ellipses are for illustration and do not represent analysis gates. Bottom: (i) Decay curve gated on the 355–285 keV γ cascade decay of the 640 keV state in ^{62}Mn. The fit of this decay curve gives a ^{62}Cr half-life of 206(5) ms. (ii) Decay curve gated on the 815–877 keV γ cascade decay of the 1692 keV state in ^{62}Fe. The fit of this decay curve gives a ^{62}Mn half-life of 112(7)ms. (iii) Total ^{62}Cr decay curve without γ gating. In each case, the total fit (black solid line), the decay of ^{62}Cr (blue dashed line), the decay of ^{62}Mn (green dashed line), the decay of the ^{62}Mn long component (purple dashed line), and the background (cyan dashed line) are shown.

Stronger constraints come from the non-observation of the γ rays reported from the decay of the long-lived β-decaying state of ^{62}Mn [2,22], in particular the 877–1299 keV cascade from the deexcitation of the 2176 keV level in ^{62}Fe. We estimate that the absence of a clear detection (Fig. 4) limits feeding of the long component to less than 20%. The lack of β-delayed neutrons from ^{62}Cr also limits feeding of the long component, as it must have a significant P_n to be detectable

in the neutron decay curve of the previous experiment [6], though this is difficult to quantify due to the inconsistencies in the obtained P_n values with other work, including this study.

C. ^{65}Fe

^{65}Fe is known to have a β-decaying high-spin isomer at 402 keV [23,24] that could potentially be coproduced along with the lower spin ground state by fragmentation. No previous experimentally measured β-delayed neutron emission branch has been reported for either the ground state or the isomer. The neutron-gated decays associated with implants of ^{65}Fe do not show any excess of neutrons above background (Fig. 6) and we can thus determine an upper limit of $P_n < 1\%$ for both the ground and isomeric states. A relatively small P_n is expected given the small Q-value windows for β-delayed neutron emission of 503(21) and 101(22) keV for the ground state and isomer, respectively.

IV. CONCLUSIONS

Our results resolve the discrepancy between the reported large P_n value for ^{64}Mn of 33(2)% obtained from a neutron long counter measurement [6], and the much smaller value of 2.6(7)% from β-delayed gamma spectroscopy [9], with the latter being deduced from the absolute intensity of the 995-keV γ ray arising from the decay of the neutron daughter ^{63}Fe. Our new result of 1.5(6)% is consistent with the smaller value, resulting in a weighted average of 2.1(4)%. This value
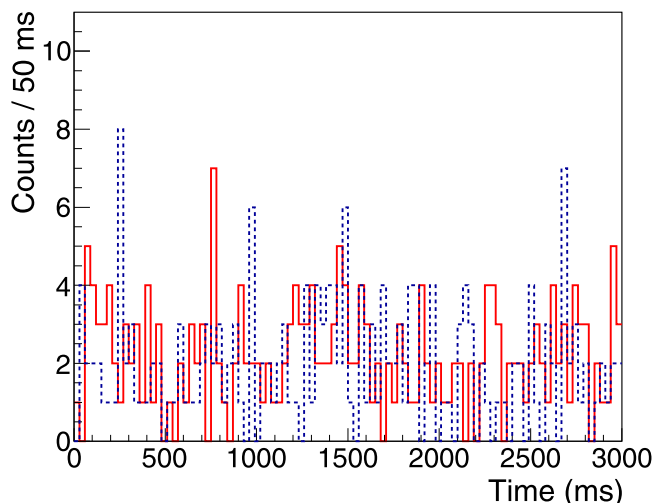
FIG. 6. Neutron-gated decay curve of ^{65}Fe (red solid histogram) and neutron-gated background (grey dashed histogram).

is slightly lower than the prediction of the global QRPA model [11] that uses a simple energy cutoff in the calculated strength function which gives a P_n of 3.1%. A more recent prediction using the same model to populate the daughter states, but employing a statistical approach to determine the final branching into neutrons or γ rays, predicts a slightly smaller value of 1% [8]. This may support the use of the statistical approach. The upper limits of 1% for the P_n values of ^{62}Cr and ^{65}Fe are also in line with expectations.

The relatively large $\beta\gamma$ statistics enables us to obtain more accurate β-decay half-lives for ^{62}Cr and the short-lived isomer

in the β daughter ^{62}Mn. In particular, our γ-gated results do not suffer from systematic errors due to parameter degeneracies in the simultaneous fitting of parent and daughter half-lives from a single β-decay curve. The new ^{62}Cr half-life is 206(5) ms, in agreement but more precise than previous measurements obtaining 187(15) ms [19] and 209(12) ms [18]. For the short lived isomer in ^{62}Fe we obtain 111(6) ms, somewhat longer but still within $(1–2)\sigma$ compared to previous work quoting 84(10) ms [6] and 93(13) ms [18]. The new constraint obtained for the P_n of ^{62}Cr enabled us to search for a possible ^{62}Cr β-decay feeding of the long-lived isomer in ^{62}Fe. Our results support the proposal put forth by the authors of [18] that longer-lived β-decaying isomer of ^{62}Mn has a high spin and is therefore not strongly populated by the β decay of ^{62}Cr (ground state $J^\pi = 0^+$). While our decay curve fit has a weak preference for nonzero population, our γ data only allow us to obtain an upper limit of 20%. Further experiments will be required to quantify the population.

[1] A. Gade and S. N. Liddick, J. Phys. G: Nucl. Part. Phys. **43**, 024001 (2016).

[2] M. Hannawald *et al.* (ISOLDE Collaboration), Phys. Rev. Lett. **82**, 1391 (1999).

[3] J. Ljungvall, A. Görgen, A. Obertelli, W. Korten, E. Clément, G. de France, A. Bürger, J.-P. Delaroche, A. Dewald, A. Gadea, L. Gaudefroy, M. Girod, M. Hackstein, J. Libert, D. Mengoni, F. Nowacki, T. Pissulla, A. Poves, F. Recchia, M. Rejmund *et al.*, Phys. Rev. C **81**, 061301(R) (2010).

[4] W. Rother, A. Dewald, H. Iwasaki, S. M. Lenzi, K. Starosta, D. Bazin, T. Baugher, B. A. Brown, H. L. Crawford, C. Fransen, A. Gade, T. N. Ginter, T. Glasmacher, G. F. Grinyer, M. Hackstein, G. Ilie, J. Jolie, S. McDaniel, D. Miller, P. Petkov *et al.*, Phys. Rev. Lett. **106**, 022502 (2011).

[5] S. N. Liddick, S. Suchyta, B. Abromeit, A. Ayres, A. Bey, C. R. Bingham, M. Bolla, M. P. Carpenter, L. Cartegni, C. J. Chiara, H. L. Crawford, I. G. Darby, R. Grzywacz, G. Gürdal, S. Ilyushkin, N. Larson, M. Madurga, E. A. McCutchan, D. Miller, S. Padgett *et al.*, Phys. Rev. C **84**, 061305(R) (2011).

[6] M. W. Hannawald, Kernspektroskopie an N=40 und N=82 nukliden, Ph.D. thesis, Johannes Gutenberg Universität Mainz, 2000.

[7] B. Singh and J. Chen, Nucl. Data Sheets **178**, 41 (2021).

[8] M. R. Mumpower, T. Kawano, and P. Möller, Phys. Rev. C **94**, 064317 (2016).

[9] D. Pauwels, D. Radulov, W. B. Walters, I. G. Darby, H. De Witte, J. Diriken, D. V. Fedorov, V. N. Fedosseev, L. M. Fraile, M. Huyse, U. Köster, B. A. Marsh, L. Popescu, M. D. Seliverstov, A. M. Sjödin, P. Van den Bergh, J. Van de Walle, P. Van Duppen, M. Venhart, and K. Wimmer, Phys. Rev. C **86**, 064318 (2012).

[10] W. W. von Seeger, P. A. DeYoung, A. Spyrou, S. Karampagia, E. F. Brown, S. Ahn, B. P. Crider, A. C. Dombos, G. W. Hitt, C. Langer, R. Lewis, S. N. Liddick, S. Lyons, Z. Meisel, F. Montes, F. Naqvi, W.-J. Ong, C. F. Persch, J. Pereira, H. Schatz *et al.*, Phys. Rev. C **109**, 044312 (2024).

[11] P. Moller, J. Nix, W. Myers, and W. Swiatecki, At. Data Nucl. Data Tables **59**, 185 (1995).

[12] J. I. Prisciandaro, A. C. Morton, and P. F. Mantica, Nucl. Instrum. Methods Phys. Res. Sect. A **505**, 140 (2003).

[13] J. Pereira, P. Hosmer, G. Lorusso, P. Santi, A. Couture, J. Daly, M. Del Santo, T. Elliot, J. Görres, C. Herlitzius, K.-L. Kratz, L. Lamm, H. Lee, F. Montes, M. Ouellette, E. Pellegrini, P. Reeder, H. Schatz, F. Schertz, L. Schnorrenberger *et al.*, Nucl. Instrum. Methods Phys. Res. Sect. A **618**, 275 (2010).

[14] W. J. Ong, Quantifying the urca cooling impact of mass 61 nuclei in x-ray bursting systems, Ph.D. thesis, Michigan State University, 2018.

[15] W. J. Ong, E. F. Brown, J. Browne, S. Ahn, K. Childers, B. P. Crider, A. C. Dombos, S. S. Gupta, G. W. Hitt, C. Langer,

R. Lewis, S. N. Liddick, S. Lyons, Z. Meisel, P. Möller, F. Montes, F. Naqvi, J. Pereira, C. Prokop, D. Richman *et al.*, Phys. Rev. Lett. **125**, 262701 (2020).

[16] B. Erjun and H. Junde, Nucl. Data Sheets **92**, 147 (2001).

[17] P. Möller, J. Nix, and K.-L. Kratz, At. Data Nucl. Data Tables **66**, 131 (1997).

[18] L. Gaudefroy, O. Sorlin, C. Donzaud, J. Angelique, F. Azaiez, C. Bourgeois, V. Chiste, Z. Dlouhy, S. Grévy, D. Guillemaud-Mueller *et al.*, Eur. Phys. J. A **23**, 41 (2005).

[19] O. Sorlin, C. Donzaud, L. Axelsson, M. Belleguic, R. Béraud, C. Borcea, G. Canchel, E. Chabanat, J. Daugas, A. Emsallem *et al.*, Nucl. Phys. A **660**, 3 (1999).

[20] E. Runte, W. D. Schmidt-Ott, P. Tidemand-Petersson, R. Kirchner, O. Klepper, W. Kurcewicz, E. Roeckl, N. Kaffrell, P. Peuser, K. Rykaczewski, M. Bernas, P. Dessagne, and M. Langevin, Nucl. Phys. A **399**, 163 (1983).

[21] A. Simon, S. Quinn, A. Spyrou, A. Battaglia, I. Beskin, A. Best, B. Bucher, M. Couder, P. DeYoung, X. Fang, J. Görres, A. Kontos, Q. Li, S. Liddick, A. Long, S. Lyons, K. Padmanabhan, J. Peace, A. Roberts, D. Robertson *et al.*, Nucl. Instrum. Methods Phys. Res. Sect. A **703**, 16 (2013).

[22] N. Hoteling, C. J. Chiara, R. Broda, W. B. Walters, R. V. F. Janssens, M. Hjorth-Jensen, M. P. Carpenter, B. Fornal, A. A. Hecht, W. Królas, T. Lauritsen, T. Pawłat, D. Seweryniak, X. Wang, A. Wöhr, J. Wrzesiński, and S. Zhu, Phys. Rev. C **82**, 044305 (2010).

[23] M. Block, C. Bachelet, G. Bollen, M. Facina, C. M. Folden, C. Guénaut, A. A. Kwiatkowski, D. J. Morrissey, G. K. Pang, A. Prinke, R. Ringle, J. Savory, P. Schury, and S. Schwarz, Phys. Rev. Lett. **100**, 132501 (2008).

[24] D. Pauwels *et al.*, Phys. Rev. C **79**, 044309 (2009).